# Multifractal Method for the Instantaneous Evaluation of the Stream Function in Geophysical Flows

Antonio Turiel,* Jordi Isern-Fontanet,† Emilio Garcia-Ladona,‡ and Jordi Font§

*Institut de Ciències del Mar, Passeig Marítim de la Barceloneta, 37-49, 08003 Barcelona, Spain*

(Received 19 November 2004; published 1 September 2005)

Multifractal or multiaffine analysis is a promising new branch of methods in nonlinear physics for the study of turbulent flows and turbulentlike systems. In this Letter we present a new method based on the multifractal singularity extraction technique, the maximum singular stream-function method (MSSM), which provides a first order approximation to the stream function from experimental data in 2D turbulent systems. The essence of MSSM relies in relating statistical properties associated with the energy cascade in flows with geometrical properties. MSSM is a valuable tool to process sparse collections of data and to obtain instant estimates of the velocity field. We show an application of MSSM to oceanography as a way to obtain the current field from sea surface temperature satellite images; we validate the result with independent dynamical information obtained from sea level measurements.

DOI: 10.1103/PhysRevLett.95.104502 PACS numbers: 47.11.+j, 47.27.Jv, 47.53.+n, 89.75.Da

The description of turbulent flows as multifractal objects is a powerful approach which has given promising results during the past two decades [1,2]. The roots of such a multiple-scaling formalism can be tracked back from the early works by Kolmogorov [3]; it was then evident that, although scale invariance was well established, a description of structure functions in terms of a single scaling exponent is impossible. Parisi and Frisch's seminal work [4] revealed the connection between the statistical properties of the flow (structure functions) and its geometrical arrangement (multifractal components). In fact, the relevant patterns and structures in the different stages of the cascade of energy in high Reynolds turbulence have been regarded as fractal components characterized by scaling exponents (singularity exponents) within a multifractal hierarchy [5]. More recently, on different physical systems where similar underlying structures exist, the use of wavelet techniques has allowed the explicit calculation of the singularity exponents at each point on experimental data of scalar and vectorial variables [6–8]. Those wavelet-based singularity detection techniques provide a very fine, accurate decomposition of the signal in the relevant patterns and structures, each one associated to a type of singularity whose main advantage is its close connection with the theory of energy cascades commonly used to describe turbulent flows [9].

Many of the past and recent work has focused on the application of such decomposition to characterize global and local statistical properties of the flows [1,10,11]. However, our approach is just the opposite: to retrieve the dynamics of flows from an incomplete and coarse signal that it is *a priori* known to have multifractal structure. Suitable signals include measurements of different variables in geophysical signals [6], in laboratory experiments on turbulent flows [10], and even in many other different contexts [12,13]. In this Letter, we will present a method based on the multifractal decomposition to retrieve a good approximation of the stream function from data on a scalar variable. In a first stage we will obtain the main stream lines from the data image which correspond to the vertex manifold in the multifractal hierarchy. Then, we will use some simple geometrical and statistical reasoning to derive from them a simple stream function, the maximum singular stream function (MSS).

Let $s(\vec{x})$ be a multifractal signal in a planar flow. We will assume that $s(\vec{x})$ is mainly advected by the flow, but not necessarily conserved (even more, difussive and/or reactive effects may be important). Our goal is to recover the advecting flow, as defined by its stream function. The first step is to assess some physically significant structures by multifractal classification. We calculate the local singularities of the signal by wavelet projecting [14] the standard multifractal measure $\mu$ defined by the gradient of $s(\vec{x})$, $d\mu(\vec{x}) = dx|\nabla s|(\vec{x})$, as in [15]. What is characteristic to multifractal signals is local power-law scaling. Such scaling is assessed using wavelet projections over an appropriate wavelet function $\Psi$, at each location $\vec{x}$ and variable scales $r$ [that will be denoted by $T_\Psi s(\vec{x}, r)$]. The signal $s$ will be multifractal if and only if $T_\Psi s(\vec{x}, r) \propto r^{h(\vec{x})}$ [8,14,16]. At each point, the local power law is completely defined by the so-called singularity exponent $h(\vec{x})$ [8,16], which, in fact, is a measure of the degree of regularity or singularity of the signal at that particular point [14]. Once every point $\vec{x}$ is assigned a singularity exponent $h(\vec{x})$, it is possible to decompose the signal into different patterns (the fractal components), classified from the most singular (usually associated to transitions) to the less singular (associated to smooth, continuous areas) [8,16]. This is one of the main advantages of multifractal formalism, because no continuity requirement is imposed and, in fact, some of the fractal components are associated to discontinuities and sharp transitions [6,8]. We are mainly interested in the most singular points in the multifractal hierarchy. From the statistical point of view, the most singular manifold (MSM) has been related with the vertex of the energy cascade [5]. In the context of signal processing, a retrieval

 

algorithm based on statistical assumptions (determinism, linearity, translational invariance, isotropy, and scale-invariant power spectrum) and taking information conveyed by the MSM only, has been proposed [17]. Then, if we denote the gradient of $s(\vec{x})$ restricted to the MSM by $\nabla_\infty s$ (that is, $\nabla_\infty s = 0$ outside the MSM), the signal can be recovered as $s = \vec{g} \otimes \nabla_\infty s$, where the symbol $\otimes$ must be understood as a convolution dot product, and the vectorial kernel $\vec{g}$ has a simple expression in Fourier space: $\hat{\vec{g}}(\vec{k}) = i\vec{k}/k^2$ [17]. This algorithm has been experimentally validated in different instances as image processing [17] and analysis of meteorological images [15], exhibiting a high performance.

The objective here is to create a stream function and not to recover data so we will not make a direct application of the formula above, but substitute $\nabla_\infty s$ by the gradient of the stream function over the MSM. In the absence of additional dynamical information, we will define the simplest gradient field which is consistent with our requirements. First of all, as the MSM represents stream lines, the gradient of the stream function must be perpendicular to these lines (so that the stream function is a conserved quantity). We will impose this perpendicularity condition, orienting our proxy gradient in the same sense as the original gradient. We would need to add some dynamical information on the speed (the modulus of the velocity), but in the absence of any model for it we will just fix it as a constant (as speed changes smoothly along a stream line, this is a good approximation). So, we fix the modulus of the gradient of our proxy stream function over the MSM to a constant value (by convention, 1, without unities, as we will not include in this derivation complementary physical information to calibrate it). The result of the application of the retrieval formula, $\psi_{\mathrm{MSS}}$, is what we call the MSS.

To test and validate the performance of the MSS to recover the original stream function we need independent measurements of both $s(\vec{x})$ and the stream function. Geophysical flows are thus a natural test ground. For instance, ocean flows are almost bidimensional due to the constraint of the rapid rotation of Earth and strong stratification; in addition, their regime is that of high Reynolds regime [18]. This quasibidimensional behavior allows the definition of a stream function, the geostrophic stream function $\psi$. The value of $\psi$ is proportional to the sea surface height (SSH), a variable which can be directly measured by satellites [19]. In addition, numerical simulations of stratified quasigeostrophic flows, more representative of geophysical fluids, show that passive tracers behave in a similar way as planar homogeneous flows [20]. Remote sensing data do not provide access to purely passive tracers, however; but there is a remotely sensed variable which can be useful—sea surface temperature (SST). In oceans and over short periods of time, temperature is rather passively advected by the strongest currents and should work as a good proxy of the stream function, at least locally. When SST and SSH maps are compared, important coincidences are usually found over areas dominated by the strongest currents. In Fig. 1 we show an example SST image and corresponding SSH map: Those images clearly show the strong signal associated to the Gulf Stream flowing close to the coast from Florida through to Cape Hatteras and then offshore, and several mesoscale eddies evidencing the characteristic spatial variability of the region [21].

In general, however, the weakest structures observed on SSH images are only faintly apparent on SST images or even completely absent. This lack of correspondence between SST and SSH can be due to many phenomena: heat injection or depletion, convective instabilities at some places, etc. What is important for us is that from all the effects modifying temperature, only diffusion modifies singularity exponents (tending to smoothen differences) and it acts at a slow rate. Recent analyses of advected reactive tracers applied to SST have shown that the multifractal patterns compare well with the patterns seen in an advected tracer [22]. So that, it is a reasonable assumption that multifractal singularities are advected by the flow. Our goal is to detect the multifractal singularities and from them to construct an ''advective temperature,'' a proxy of SST that represents what surface temperature should be in the presence of pure horizontal advection.

We have applied our methodology to obtain the MSS from the SST record shown in Fig. 1. As stated in the introduction, we process the measure $\mu$ instead of the signal $s$ itself because low-order wavelets provide better control on the log-log regressions used to compute singularities (see discussion in [7]); in addition, the spatial localization is improved when the number of zero crossings in the wavelet is reduced [23]. We used a wavelet $\Psi(\vec{x}) = \frac{1}{(1+\vec{x}^2)^2}$, which provides both a wide enough detection range [16,23] and good spatial localization. The experimental range of singularities was $(-1.16, 0.90)$, with 75% of points having log-log regressions with a regression coefficient above 0.9. As we deal with a physical signal, it is uniformly bounded [24] and so the minimum theoretical possible value for the singularities is $-1$, which is in close agreement with our results, accepting an experimental uncertainty of $\sim 0.16$ at least (which is in agreement with what has been observed in other works). In addition, values close to $-1$ are induced by the boundaries and almost all of

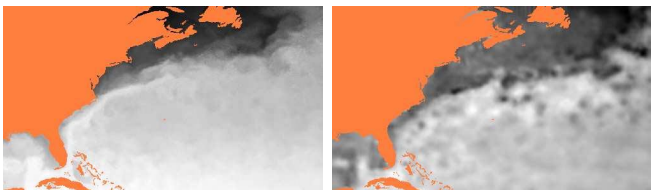

FIG. 1 (color online). Left: SST image from composite of AVHRR [19] images acquired 31st December, 2003. The covered area goes from 270° to 320° E, and from 20° to 50° N. Right: SSH map for the same region and time combining data from the Jason and ENVISAT satellite altimeters, [19,31].

them can be found at the limits of the image and the coast. A typical value for most bulk (nonboundary) singular points is around $-0.5$. In Fig. 2 we can see a determination of the MSM at a given level of quantization. This set consists of well-defined stream lines, which is quite reasonable if we take into account that streams shear the flow creating sharp local behavior, a singularity. Notice that singularities are calculated locally, and for that reason the appearing lines need not be evident when looking at the whole image (large gradients), but when examining their neigborhood (large gradients compared to those of the surroundings). For that reason, we can detect stream lines that normally will be masked by long-range effects and with relatively small gradients. Then the stream function is reconstructed as described before. The result (the MSS) is shown in the same Fig. 2; in addition we present in Fig. 3 a closer inspection of MSS compared to the level curves of SSH. The improvement implied by MSS in the determination of the fine structure in altimetry is really outstanding.

The visual assessment of the MSS provides good correspondence with the data provided by SSH, but this qualitative assessment is not enough to validate the methodology. We thus need to define some quantitative, objective measures of the quality of the MSS, based on its closeness to the SSH record. The level of closeness between both functions will be, however, quite limited by some processing issues. On one hand, we are dealing with images that have been generated after heavy preprocessing techniques. In the case of SSH, only some satellite traces are known and from them the whole field is interpolated, with some post processing and low-pass filtering. In the case of SST, the used data have been temporally and spatially interpolated to eliminate voids (typically from clouds). In addition, we need to compare data acquired at different spatial resolutions; we solve this problem by zero padding the higher frequencies of SSH until reaching the greater resolution of SST, but this interpolation scheme induces smoother gradients on the SSH. Anyway, the relevant mesoscale phenomena are evident in both images, as the visual inspection reveals, and any reasonable quantitative measure should put in evidence this coincidence.

A first measure is given by the amount of advective derivative induced by one velocity field over the other. We will denote by $\psi_a$ the SSH and by $\psi_{\mathrm{MSS}}$ the MSS. Each stream function induces a velocity field, $\vec{v}_a = \nabla_\perp \psi_a$ and $\vec{v}_{\mathrm{MSS}} = \nabla_\perp \psi_{\mathrm{MSS}}$. The total time derivative of $\psi_{\mathrm{MSS}}$ under the current field induced by $\psi_a$ is given by $\frac{d\psi_{\mathrm{MSS}}}{dt} = \frac{\partial \psi_{\mathrm{MSS}}}{\partial t} + \vec{v}_a \cdot \nabla \psi_{\mathrm{MSS}}$. The second summand represents the advective derivative of one stream function with respect to the other, and it is antisymmetric with respect to field exchange: $\vec{v}_a \cdot \nabla \psi_{\mathrm{MSS}} = \nabla_\perp \psi_a \cdot \nabla \psi_{\mathrm{MSS}} = -\nabla_\perp \psi_{\mathrm{MSS}} \cdot \nabla \psi_a = -\vec{v}_{\mathrm{MSS}} \cdot \nabla \psi_a$. We can compare the total amount of advective derivative with the product of kinetic energies to obtain the adimensional ratio $\rho_{a,\mathrm{MSS}}$ defined as $\rho_{a,\mathrm{MSS}} = \frac{\int d\vec{x} |\nabla_\perp \psi_a \cdot \nabla \psi_{\mathrm{MSS}}|}{\sqrt{\int d\vec{x} |\nabla \psi_a|^2 \int d\vec{x} |\nabla \psi_{\mathrm{MSS}}|^2}}$. By Minkowski's inequality, $\rho \leq 1$; $\rho = 1$ only when the two fields are completely mutually perpendicular and $\rho = 0$ when they are perfectly aligned, that is, when both stream functions share the same stream lines. For the case shown in this Letter, we obtain $\rho_{a,\mathrm{MSS}} = 0.099$, which can be considered as a sign of good coincidence between their stream lines. However, the same measure directly comparing SST with SSH returns a value which is even better, $\rho_{a,\mathrm{SST}} = 0.019$. This is because the SST has wide regions with very small gradients which almost do not contribute to $\rho_{a,\mathrm{SST}}$, and then its value is dominated by the very good correspondence of the thermal front of the Gulf Stream, disregarding the contribution of all the other points. But the SST is a poor template for the stream function precisely because of the abundance of faint gradients, which lead to poorly defined stream lines. In contrast, the MSS has a much more uniform distribution of gradients, well-defined stream lines, and a reasonably good alignment with the SSH velocity field.

A second test consisted in obtaining the level sets for the assessed function (i.e., MSS and SST, respectively), and measure the variability of the altimetric data along them. If the level sets of the tested function coincide with the stream lines of SSH, SSH should be constant along those level sets. We measured the sum of variances of SSH along the different level sets, each one weighted with its length. We obtained the level sets by quantizing the dynamic range of the tested function over 25 levels, then separating the

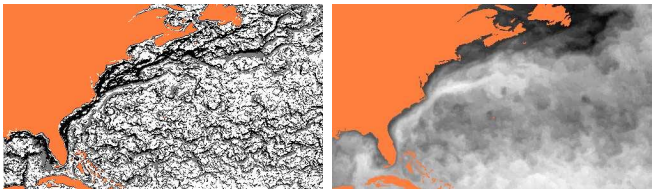

FIG. 2 (color online). Left: 33% most singular points. Right: stream function (MSS) derived from the most singular points.

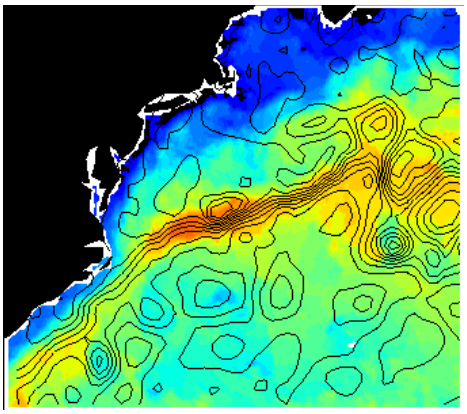

FIG. 3 (color online). Detail of the comparison: we show the level sets from altimetry overimposed to a color representation of the MSS.

different connected components. The total variance of the altimetric signal for the studied image was 164 $cm^2$. The sum of variances of SSH along the MSS level sets was 4.2 $cm^2$ (2.6% of the total). The sum of variances of SSH along the SST level sets was 15.5 $cm^2$ (9.4% of the total). We see that MSS level sets give a better estimation than those of SST about the actual stream lines.

Our results indicate that the obtained MSS share to a good extent the stream lines with those of SSH. We have not exhaustively tested our methodology due to the lack of good quality SSH records, although we have carried out a few additional tests in different regions and dates with comparable results (Additional examples are available [25]).

In the context of geophysical flows, the example shown here is a direct application to retrieve quasisynoptic velocity fields as an alternative to several existent techniques [26–29]. All those methods rely on imposing strong continuity conditions in both space and time, having a steady enough time sequence of well-defined patterns to be tracked and, even more important, they are not based on a standard notion of the physically relevant patterns. In addition, those methods may fail for some configurations of the flow regime. On the contrary, the method presented here is based on intrinsic physical properties of the flow (its multifractal structure) and, additionally, furnishes a good detection technique.

MSSM can be generalized, at least partially, to higher dimensional contexts. For instance, 3D multifractal systems are also organized in multifractal singularity components, so the first steps of MSSM proceed in the same way: detection and construction of the advective proxy. This proxy cannot be interpreted as a stream function any longer, but its level sets are union of stream lines. Some additional information would then be required, for instance extra field information on local speeds (density gradients, *in situ* velocity measurements, etc.).

But the technique presented here goes beyond its applications' turbulent flows. The methodological basis has its roots in the existence of a multifractal/multiscaling hierarchy, so potentially it is of application in any dynamical system possessing such structure. Systems of this kind range from econometric time series [12] to natural image statistics [30] and heart-beat time series [13], among possibly many other.

This is a contribution to IMAGEN (Spanish R+D Plan: REN2001-0802-C02-02) and MERSEA projects (EU AIP3-CT-2003-502885). A. Turiel is contracted under the Ramon y Cajal program by the Spanish Ministry of Education. J. Isern-Fontanet is funded by the IMAGEN and MERSEA projects. The altimeter products were produced by Ssalto/Duacs and distributed by AVISO with support from CNES.

*Electronic address: turiel@icm.csic.es
†Electronic address: jisern@icm.csic.es
‡Electronic address: emilio@icm.csic.es
§Electronic address: jfont@icm.csic.es

[1] K. Sreenivasan, Annu. Rev. Fluid Mech. **23**, 539 (1991).
[2] U. Frisch, *Turbulence* (Cambridge University Press, Cambridge, England, 1995).
[3] A. Kolmogorov, Doklady Seriia biologiia/Akademii nauk SSSR **32**, 141 (1941).
[4] G. Parisi and U. Frisch, in *Turbulence and Predictability in Geophysical Fluid Dynamics*, Proceedings of the International School of Physics "Enrico Fermi," edited by M. Ghil, R. Benzi, and G. Parisi (North-Holland, Amsterdam, 1985), p. 84.
[5] Z. S. She and E. Leveque, Phys. Rev. Lett. **72**, 336 (1994).
[6] J. Arrault, A. Arneodo, A. Davis, and A. Marshak, Phys. Rev. Lett. **79**, 75 (1997).
[7] Z. R. Struzik, Fractals **8**, 163 (2000).
[8] A. Turiel and N. Parga, Neural Comput. **12**, 763 (2000).
[9] B. Dubrulle, Phys. Rev. Lett. **73**, 959 (1994).
[10] A. Arneodo *et al.*, Europhys. Lett. **34**, 411 (1996).
[11] T. Arimitsu and N. Arimitsu, J. Phys. Condens. Matter **14**, 2237 (2002).
[12] B. B. Mandelbrot, A. Fisher, and L. Calvet, Cowles Foundation Discussion Paper No. 1164 (Yale University, New Haven, CT, 1997).
[13] L. A. N. Amaral, A. L. Goldberger, P. C. Ivanov, and H. E. Stanley, Phys. Rev. Lett. **81**, 2388 (1998).
[14] I. Daubechies, *Ten Lectures on Wavelets* (Capital City Press, Montpelier, VT, 1992).
[15] J. Grazzini, A. Turiel, and H. Yahia, in *Proceedings of ICPR 2002, Vol. 3* (IEEE, Los Alamitos, CA, 2002), p. 764.
[16] A. Arneodo *et al.*, *Ondelettes, Multifractales et Turbulence* (Diderot Editeur, Paris, France, 1995).
[17] A. Turiel and A. del Pozo, IEEE Transactions on Image Processing **11**, 345 (2002).
[18] P. Rhines, Annu. Rev. Fluid Mech. **11**, 401 (1979).
[19] SST: http://www.ifremer.fr/las/servlets/dataset; SSH: http://las.aviso.oceanobs.com/las/.
[20] A. Bracco, J. von Hardenberg, A. Provenzale, J. Weiss, and J. McWilliams, Phys. Rev. Lett. **92**, 084501 (2004).
[21] L. Fu, J. Vazquez, and M. Parke, J. Geophys. Res. **92**, 749 (1987).
[22] E. Abraham and M. Bowen, Chaos **12**, 373 (2002).
[23] A. Turiel and C. Pérez-Vicente, in *Proceedings of J. D'étude Sur les Méthodes Pour les Signaux Complexes en Traitement D'image*, edited by H. Yahia, I. Herlin, and A. Turiel (INRIA, Rocquencourt, France, 2004), p. 41.
[24] S. Mallat, *A Wavelet Tour of Signal Processing* (Academic, New York, 1999), 2nd ed.
[25] http://www.icm.csic.es/geo/gof/projects/imagen/mssm/.
[26] J. Wilkin, M. Bowen, and W. Emery, Ocean Dynamics **52**, 95 (2002).
[27] Q. X. Wu, D. Pairman, S. J. McNeill, and E. J. Barnes, IEEE Transactions on Geoscience and Remote Sensing **30**, 166 (1992).
[28] A. Liu, S. Martin, and R. Kwok, J. Atmos. Ocean. Technol. **14**, 1187 (1997).
[29] D. Béréziat and J. Berroir, Env. Mod. Sys. **15**, 513 (2000).
[30] A. Turiel, G. Mato, N. Parga, and J. P. Nadal, Phys. Rev. Lett. **80**, 1098 (1998).
[31] P. L. Traon, F. Nadal, and N. Ducet, J. Atmos. Ocean. Technol. **15**, 522 (1998).